Discontinuous Crack Growth of Polyimide Resin,

Effect of Molecular Weight

M. Notomi[1], K. Kishimoto[2], T. Shibuya[2], H. Inaba[3] and A. Morita[3]

[1]Department of Mechanical Engineering, Meiji University, 1-1-1 Higashimita, Tama-ku, Kawasaki, Kanagawa, 214-8571, JPN
[2]Graduate School of Science and Engineering, Tokyo Institute of Technology, 2-12-1, O-okayama, Meguro-ku, Tokyo, 152-8552, JPN
[3]Mitsui Chemical Co.Ltd., 1190, Kasama-Cho, Sakae-ku, Yokohama, Kanagawa, 247-8567, JPN

ABSTRACT

The effects of molecular weight on fatigue crack propagation of polyimide (PI) are investigated for four kinds of molecular weight (Mw) from 2.5×10^4 g/mol to 3.8×10^4 g/mol. The rate of fatigue crack growth follows the Paris law under the ΔK range tested, and decreases with the increase of Mw. Except for the highest Mw case, the discontinuous crack growth (DCG) bands were observed on the fracture surfaces under lower ΔK. The width of DCG bands is almost independent of ΔK and increases with increase of Mw. The number of cycles needed to form one DCG band increases with increase of Mw, which is cause of the higher fatigue resistance for higher Mw. The critical values of craze stress at the onset of crack jump in DCG are estimated by Dugdale's model and are smaller for higher Mw. This result suggests that materials with higher Mw sustain more damage accumulation.

KEYWARDS

Discontinuous Crack Growth, Polyimide, Fatigue, Crack Propagation, Molecular Weight, SEM observation

INTRODUCTION

Polyimide (PI) is one of most useful engineering plastics and we have already investigated the effect of molecular weight on some mechanical properties, e.g. Young's modulus, J_{IC} and so on [1]. For applying the structural components, the behavior of fatigue crack propagation (FCP) of PI might be estimated. In some polymers, the crack does not propagate on one load cycle in spite of following the Paris law. This FCP process is called as discontinuous crack growth (DCG) [2]. For instance, Takemori [3] has investigated the DCG mechanism of amorphous polymer, e.g. PC. Although he indicated that this behavior occurs as a consequence of both crazing and shear banding ahead of the crack tip, there is little consideration about the width of DCG. While, Skibo [4] studied the fatigue ... of DCG bands was the same as the length of craze regio... ct of molecular weight on the FCP of PI and discussed t...

METHOD

Table 1 Material properties of specimens.

Type	Molecular weight [g/mol]	Young's modulus [GPa]	Tensile strength [MPa]	Poisson's ratio	J_{IC} [kN/m]
A	2.5×10^4	3.18	88.3	0.395	3.6
B	2.8×10^4	2.98	88.3	0.399	5.7
C	3.0×10^4	3.14	86.6	0.390	6.6
D	3.8×10^4	3.68	110.0	0.382	7.8

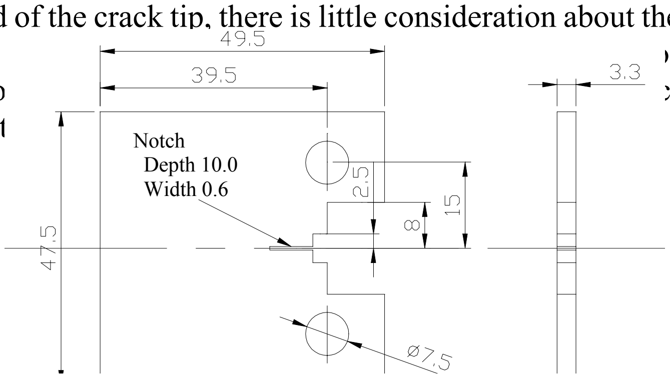

Fig. 1 Dimensions of CT specimen.

Thermoplastic polyimides with four kinds of molecular weight are used. They are called as Type A, B, C and D for convenient. Table 1 shows molecular weight, Young's modulus, tensile strength and elastic-plastic fracture toughness, J_{IC} of these material [1]. The dimensions of compact tension specimen are shown in Figure 1, which is cut from the plate made by the injection molding. An initial notch with 0.6 mm width is introduced by a precision cutting blade machine.

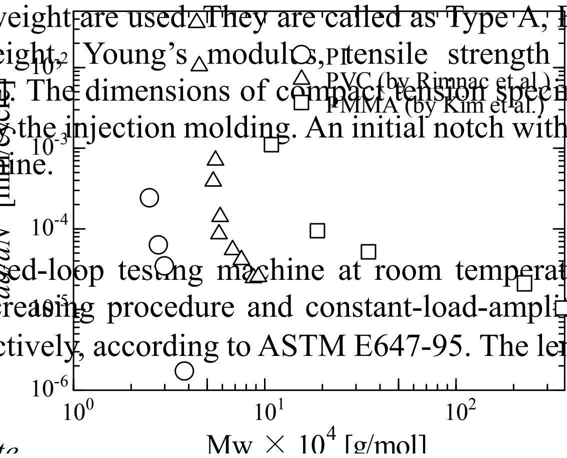

Fig.3 The effect of molecular weight on *da/dN* at ΔK = 0.7 MPam$^{1/2}$. Those of PVC by Rimnac et

Procedure

Fatigue tests were performed with electrohydraulic closed-loop testing machine at room temperature. Frequency was 7.5Hz and stress ratio R was 0.1. K-decreasing procedure and constant-load-amplitude procedure were applied at the lower and higher ΔK, respectively, according to ASTM E647-95. The length of crack was measured with a traveling microscope.

Stress Intensity Factor Range and Crack Propagation Rate

Stress intensity factor range ΔK is calculated by,

$$\Delta K = \frac{\Delta P}{BW^{1/2}} f(\alpha)$$

$$f(\alpha) = \frac{(2+\alpha)(0.886 + 4.64\alpha - 13.32\alpha^2 + 14.72\alpha^3 - 5.6\alpha^4)}{(1-\alpha)^{3/2}} \quad (2)$$

$$\alpha = a / W \quad (3)$$

where ΔP, B, W and a are the range of load, the thickness and the width of specimen and the length of crack, respectively.

The crack propagation rate *da/dN* is obtained as follows,

$$\left(\frac{da}{dN}\right)_{\bar{a}} = \frac{a_{i+1} - a_i}{N_{i+1} - N_i} \quad (4)$$

where a_i and N_i are the crack length and the number of load cycle on i th. In addition, the average crack length, $\bar{a} = (a_{i+1} + a_i)/2$ is used to obtain ΔK.

RESULTS and DISCUSSION

Fatigue crack propagation properties

The relationship between the ΔK and *da/dN* are shown in Figure 2 and satisfy the Paris law:

$$\frac{da}{dN} = C(\Delta K)^m \quad (5)$$

where C and m are material constants and are given in Table 2. The fatigue crack extension resistance increases with the increase of Mw. The values of *da/dN* at $\Delta K = 0.7\ \mathrm{MPa}\sqrt{\mathrm{m}}$ are shown in Figure 3. The value for type D is estimated by the extrapolation of the measured data. For the comparison, the results of PVC by Rimnac[5] and PMMA by Kim[6] are also shown in the figure. It can be seen that the fatigue properties of PI is excellent.

SEM observation

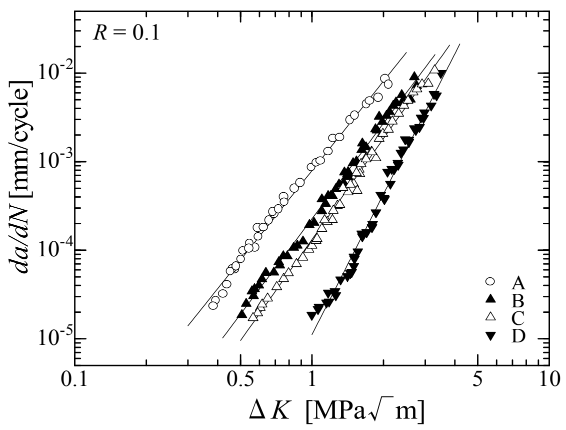

Fig. 2 Influence of molecular weight on fatigue crack propagation.

The typical fracture surfaces of type B by scanning electron microscope (SEM) are shown in Figure 4. The cracks on all photos propagate from bottom to top. Figure 4(d) indicates the observation point of each photo on the Δ*K*-*da/dN* relation. The typical DCG bands of PI are shown in Figure 4(a). In Figure 4(b) the DCG bands disappear with the advance of the crack. This is the transition of the fracture process from DCG to continuous crack growth (CCG). Since the width of DCG bands is almost constant during the process, the width might be almost independent of Δ*K*. (Please take care the different of mag nification

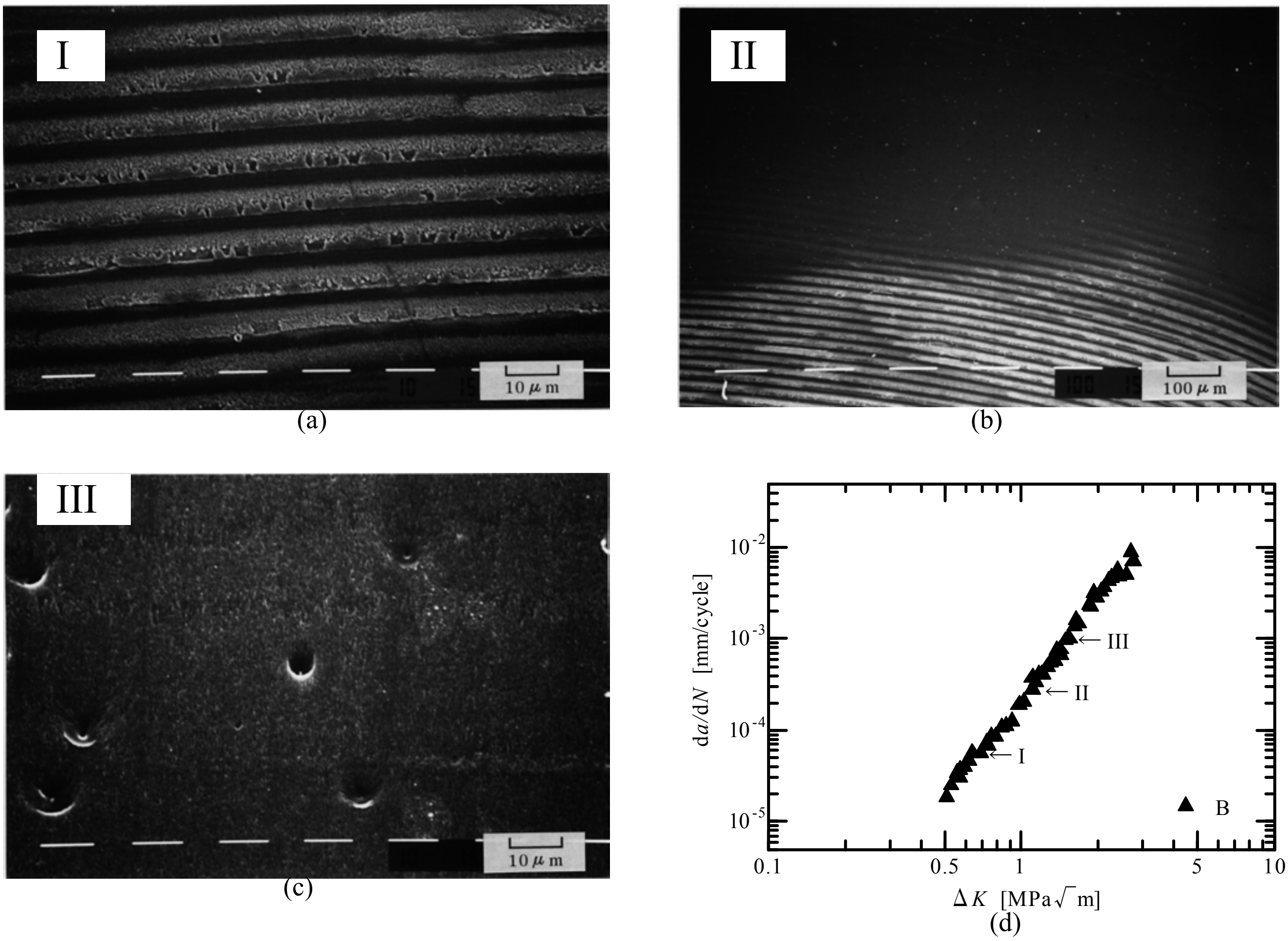

Fig. 4 SEM fractograph showing the DCG (a), the transition from DCG to FCP process (b) and the FCP process(c). The diagram (d) shows the observation point on Δ*K*-*da/dN* relation for each photo.

Table 2 Coefficients of Paris law for each specimen.

Type	A	B	C	D
C	7.93×10^{-4}	2.27×10^{-4}	1.32×10^{-4}	1.12×10^{-5}
m	3.35	3.58	3.79	5.26

Table 3 The space of DCG bands and the number of loading cycles for making DCG band. In addition, the critical fracture craze stress is derived from the Dugdale model.

Type	DCG band spacing [μm]	Number of Cycles	σ_c [MPa]
A	3.6	10	231
B	8.6	100	150
C	9.2	240	145

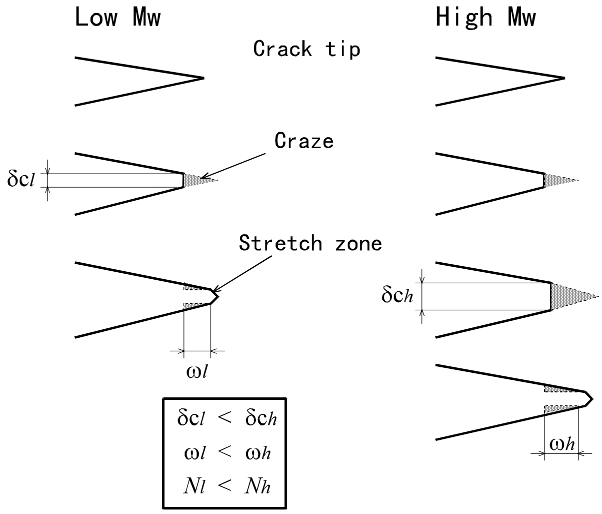

Fig. 5 Schematic diagram showing the discontinuous crack growth in each Mw.

between photos (a) and (b).) Any striation can't be seen on the fracture surface during CCG as shown in Figure 4(c). These behaviors are the same as that of type A and C. While, the morphology of the type D fracture surface is different from the others and DCG bands can't be seen on the any fracture surfaces.

Discontinuous Crack Growth

Several studies [4,6,7] have shown that the Dugdale formulation,

$$\omega = \frac{\pi}{8} \frac{\Delta K^2}{\sigma_C^2} \tag{5}$$

gives the relationship between the critical fracture craze stress σ_c at the crack jump due to damage accumulation and the width of DCG bands ω. The ω at $\Delta K = 0.7\ \mathrm{MPa}\sqrt{\mathrm{m}}$ measured by the SEM photos, the number of cycle for a crack jump and σ_c by Eq. (5) are shown in Table 3. The ω increases with the increase of Mw. Figure 5 shows a schematic figure of the craze region of a DCG band. With the increase of Mw the more damage accumulates at the craze region of the higher Mw specimen for a crack jump. Subsequently, the craze region can be extended at crack tip, that is $\omega_h > \omega_l$. While, σ_c decreases with the increase of Mw because of this damage accumulation. This decrease of σ_c needs the more number of cycles for a crack jump, that is $N_h > N_l$. Consequently, *da/dN* decreases with the increase of Mw.

REFERENCES

1. Notomi, M. Kishimoto, K. Shibuya, T. Inaba, H. and Morita, A. (1999). *Tran. Jap. Soc. Mech. Engineers,* A, **65**, 629, pp.67-71. (in Japanese)
2. Hertzberg, R. W. (1996). *Deformation and Fracture Mechanics of Engineering Materials 4th ed.*, John Willy & sons, New York.
3. Takemori, M. T. (1990). *Advances in Polym. Sci.* 91/92 pp. 263-300.
4. Skibo, M. D. Hertzberg, R. W. Manson, J. A. (1976). *J. Mater. Sci.* 11, pp. 479-490.
5. Rimnac, C. Manson, J. A. Hertzberg, R. W. and Skibo, M. D. (1981). *J. Macromol. Sci. Phys.* B19 3, pp. 351-375.
6. Kim, S. L. Skibo, M. Manson, J. A. and Hertzberg, R. W. (1977). *Polym. Eng. Sci.* 17 3, pp. 194-203.
7. Clark, T. R. Hertzberg, R. W. and Mohammadi N. (1993). *J. Mater. Sci.* 28, pp. 5161-5168.